THE JOURNAL OF PHYSICAL CHEMISTRY A LETTERS

2009, *113,* 8823–8825
Published on Web 07/10/2009

Interactions of Cl^- and OH Radical in Aqueous Solution

Marat Valiev,*,† Raffaella D'Auria,‡ Douglas J. Tobias,‡ and Bruce C. Garrett†

William R. Wiley Environmental Molecular Sciences Laboratory and Fundamental and Computational Sciences Division, Pacific Northwest National Laboratory, P.O. Box 999, Richland, Washington, 99352, and Department of Chemistry and AirUCI, University of California, Irvine, California 92697

Received: April 20, 2009; Revised Manuscript Received: June 5, 2009

There is a considerable controversy surrounding the nature of the Cl^-/OH complex in aqueous solution, which appears as a byproduct of the irradiation of salt solutions in nuclear reactor operation, radioactive waste storage, medicine, and environmental problems. In this work, we report results of combined quantum mechanical molecular mechanics calculations of ground-state free-energy surfaces and absorption spectrum through the CCSDT level of theory that are consistent with the experimental data and suggest that hemibonded $HOCl^-$ species may indeed exist in bulk aqueous solution.

Fundamental understanding of anion−radical interactions in the aqueous phase is of significant relevance to many important applications. A byproduct of irradiation of salt solutions, such species are encountered in a wide range of problems including nuclear reactors, radioactive waste storage, and medicine. As suggested by pulse radiolysis studies,[1] reaction between an OH radical and Cl^- in solution can lead to the production of Cl_2^-. A similar process in the interfacial environment has been implicated in the production of molecular chlorine from sea salt aerosol, which ultimately could lead to enhanced ozone levels in the marine boundary layer.[2,3] A detailed understanding of this reaction is hindered by uncertainty regarding the nature of the complex between OH and Cl^- in aqueous environments. Pulse radiolysis studies of sodium chloride solutions[1] and electron spin resonance (ESR) measurements on irradiated chloride hydrates[4] suggest that Cl_2^- is produced via a hemibonded HO−Cl^- species

$$H^+ + HO{-}Cl^- \rightarrow Cl^\bullet + H_2O \quad (1)$$

$$Cl^\bullet + Cl^- \rightarrow Cl_2^- \quad (2)$$

Such a mechanism, however, is not favored by gas-phase measurements[5] and ab initio simulations,[5−7] including those in bulk and interfacial aqueous environments.[7] There, the suggested pathways are based exclusively on the hydrogen-bonded OH···Cl^- complex as[3]

$$2(OH\cdots Cl^-) \rightarrow Cl_2 + 2OH^- \quad (3)$$

or[7]

$$OH\cdots Cl^- + Cl^- \rightarrow Cl_2^- + OH^- \quad (4)$$

$$Cl_2^- + OH \rightarrow Cl_2 + OH^- \quad (5)$$

The potential drawback with reaction 3 is the low probability[7] for the encounter of two OH···Cl^- complexes, while in reaction 4, the charge repulsion between two Cl anions has to be overcome.[7]

It is safe to say that the nature of the complex between OH and Cl^- remains the subject of considerable controversy. The results from prior ab initio simulations[7] based on density functional theory (DFT) showed a great sensitivity to the choice of the exchange−correlation functional, suggesting the need for more accurate treatments. The experimental absorption spectrum of Cl/OH^- was recorded by Jayson, Parsons, and Swallow[1] through pulse radiolysis experiments on aqueous sodium chloride solutions. To date, however, these measurements have not been used to test theoretical predictions of the structure. Here, we report high-level ab initio quantum mechanical molecular mechanics (QM/MM) calculations of ground and excited states of the OH/Cl^- complex in aqueous solution that are consistent with the experimental spectrum and suggest that the species observed in bulk aqueous solution may, in fact, be the hemibonded HO−Cl^- complex commonly assumed.

To ensure accurate description of electron correlation effects, our quantum mechanical (QM) treatment extends to the coupled cluster level of theory with full triples (CCSDT).[8−10] Analysis of the free-energy surface shows a stable HO−Cl^- complex only slightly higher in energy than its hydrogen-bonded counterpart, OH···Cl^-. The HO−Cl^- complex exhibits a hemibonded molecular structure with calculated 0.3 excess spin density on Cl, which is consistent with the ESR measurements.[4,6] The calculated 346 nm absorption peak of HO−Cl^- is also in good agreement with the 350 nm experimental estimate,[1] serving as an additional indicator for the presence of such a complex in the aqueous phase.

Our calculations utilize the multilevel QM/MM framework implemented in NWChem.[11−13] We investigated the system

* To whom correspondence should be addressed. E-mail: marat.valiev@pnl.gov.
† Pacific Northwest National Laboratory.
‡ University of California, Irvine.

10.1021/jp903625k CCC: $40.75

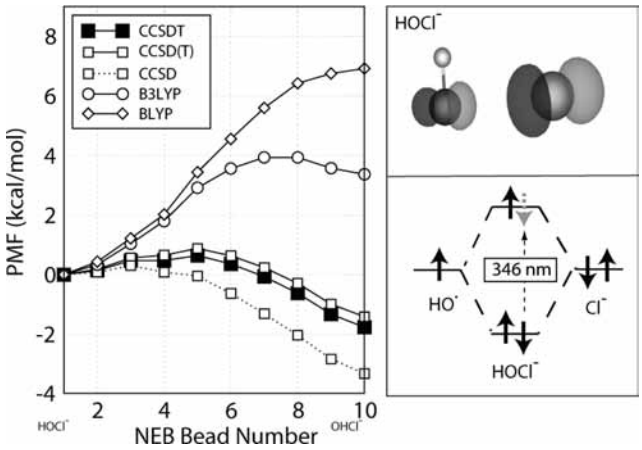

Figure 1. (left) Free-energy profile along the reaction pathway connecting HO−Cl⁻ (point 1) and OH···Cl⁻ (point 10) complexes; (top right) structure of the HO−Cl⁻ complex with the corresponding highest singly occupied molecular orbital; (bottom right) illustration of the hemibonded structure of HO−Cl⁻ showing an orbital transition corresponding to 346 nm absorption.

containing the $[OHCl]^-$ complex treated quantum mechanically in a 20 Å cubic box of classical waters described by the SPC/E[14] model. The van der Waals parameters for Cl[15] and OH[16] were chosen from prior simulations of these systems.[15,16] Most of the work was performed at the DFT/B3LYP QM/MM level of theory, which also served as a reference for coupled cluster descriptions. Optimizations and free-energy calculations were performed with the 6-31+G*[17] basis set. Calculations of the absorption spectrum were based on aug-cc-pvdz and aug-cc-pvtz[18] basis sets. Electrostatic potential (ESP) charge representation of the QM region was used to expedite QM/MM optimizations, solvent equilibration, nudged elastic band (NEB)[19] reaction pathway calculations, and free-energy calculations. The free-energy contribution from the ESP/MM representation was evaluated following the same exact finite difference thermodynamic perturbation protocol described in our previous work.[12,13] Similar to the QM+FEP approach,[20] the QM contribution to the free-energy profile at various levels of theory was approximated as an internal energy of the QM region.[11−13]

The starting point for our simulations was investigation of the covalently bound HO−Cl⁻ complex. An initial guess for this structure came from DFT/B3LYP optimization of a partially solvated model OH···Cl⁻ complex which had undergone spontaneous conversion to HO−Cl⁻. The latter structure was reoptimized in bulk solution at the B3LYP/MM level of theory through a sequence of steps involving initial relaxation, solvent equilibration to room temperature over 40 ps molecular dynamics simulations, and final optimization. The end result was a stable HO−Cl⁻ complex with a Cl−O distance of 2.46 Å and a H−O−Cl angle of 89° (see Figure 1). Additional optimization with a larger QM/MM partitioning scheme involving QM treatment of 21 additional waters around $ClOH^-$ did not affect the stability of the complex and resulted in a small change to the H−O−Cl angle (86°). As suggested by prior calculations,[6,7] we observe the formation of the hemibonded molecular structure precipitated by the interactions between the doubly occupied p orbital on Cl⁻ and the singly occupied p orbital on the OH radical (see Figure 1). This leads to a partial transfer of charge density from Cl⁻ to the OH radical, resulting in the 0.3 excess spin density on Cl, which is consistent with the ESR data.[4,6]

The hydrogen-bonded OH···Cl⁻ complex was determined through a series of constrained optimization cycles at the same B3LYP/MM level of description. The procedure involved gradual lengthening of the Cl−O distance starting from the optimized HO−Cl⁻ structure through harmonic constraints. In the final optimization step, the constraint was lifted, leading to a stable nearly linear hydrogen-bonded OH···Cl⁻ complex characterized by a Cl−H−O angle of 177° with Cl−O and Cl−H distances of 1.98 and 2.98 Å, respectively. Compared to covalently bound HO−Cl⁻, the extra electron is now fully localized on Cl, leaving the unpaired electron on OH.

To estimate the relative stabilities of the two complexes in a room-temperature aqueous solution, we calculated free-energy profiles over the reaction pathway connecting the optimized HO−Cl⁻ and OH···Cl⁻ structures. The reaction pathway was generated using a 10-point NEB B3LYP/MM calculation.[11] It is characterized by the simultaneous stretch of the Cl−O distance and rotation of the OH group toward Cl. The two competing factors that define the shape of the free-energy profile are the internal QM energy of the electronic degrees of freedom and the solvation energy reflecting the presence of the aqueous environment. Calculated at the ESP/MM level, the solvation energy of HO−Cl⁻ is 8.5 kcal/mol lower than that of OH···Cl⁻, which can be rationalized on the basis of its smaller size and partial charge transfer to the OH. The OH···Cl⁻, however, has a lower internal QM energy, the main reason why HO−Cl⁻ does not exist in the gas phase. It so happens in this case that the absolute values of the two contributions are close to each other, leading to extreme sensitivity of the total free-energy profile to the accuracy of the QM treatment (see Figure 1). For example, in the BLYP/MM description, the internal QM energy stabilization of OH···Cl⁻ (−1.59 kcal/mol) cannot overcome the lower solvation energy of HO−Cl⁻, leading to the instability of the OH···Cl⁻, which is in agreement with prior calculations.[7] The stability of OH···Cl⁻ is restored at the B3LYP/MM level; however, it remains higher in free energy than HO−Cl⁻ by 3.3 kcal/mol. The situation is reversed at the CCSD/MM level of theory, where the OH···Cl⁻ becomes lower in energy by 3.3 kcal/mol. The results start to converge at the CCSD(T)/MM and CCSDT/MM levels, where the free-energy differences between HO−Cl⁻ and OH···Cl⁻ are 1.4 and 1.7 kcal/mol, respectively. The zero-point energy vibrational and rotational contributions for the QM regions calculated at the B3LYP/MM level results in a minor stabilization of HO−Cl⁻, placing it 1.1 kcal/mol above OH···Cl⁻ at the CCSDT/MM level of theory. Overall, the main reason for the small energy difference between hemibonded and hydrogen-bonded structures comes from subtle interplay between solvation energy that favors HO−Cl⁻ and internal QM energy that favors OH···Cl⁻.

Given the availability of the experimental absorption spectrum,[1] further insight into the nature of $[OHCl]^-$ in aqueous solution can be obtained from excited-state calculations. In this case, it proved to be necessary to go up to the EOMCCSDT/MM level of theory for reliable results. EOMCCSDT/MM calculations with the aug-cc-pvdz basis set showed that the OH···Cl⁻ complex has two relatively weak absorption bands at 326 and 480 nm with 7×10^{-3} and 10^{-3} oscillator strengths, respectively. For comparison, the same calculation at the lower EOMCCSD level of theory resulted in 284 and 447 nm excited-state energies with essentially the same oscillator strengths. The use of the aug-cc-pvdz basis set appears to be adequate in this case as the EOMCCSD calculation with a bigger aug-cc-pvtz basis set showed only the slightly lower value for the first state (278 nm) while the second state remained at 447 nm. In the gas phase, EOMCCSD/aug-cc-pvdz calculations for the same OH···Cl⁻ structure show the absorption bands at 349 and 545

nm with 7×10^{-2} and 10^{-4} oscillator strengths, respectively. The covalent $HO-Cl^-$ complex, at the EOMCCSDT/MM level of the theory with aug-cc-pvdz basis set, has a strong absorption band at 346 nm with 0.26 oscillator strength involving transition within the hemibonding orbitals, as shown in Figure 1. The effect of inclusion of triples is less pronounced here as the EOMCCSD/MM calculations with aug-cc-pvdz and aug-cc-pvtz basis sets showed 339 and 345 nm values, respectively. In the gas phase, EOMCCSD/aug-cc-pvdz calculations for the same $HO-Cl^-$ structure show the dominant absorption band at 380 nm with 0.29 oscillator strength. Overall, the absorption spectrum of $HO-Cl^-$ is consistent with experimental data[1] and seems to provide the closest agreement with the experimental absorption peak at 350 nm.[1]

Structural optimizations, free-energy calculations, and analysis of the absorption spectrum performed in this work provide substantial evidence toward the existence of a hemibonded $HO-Cl^-$ complex in aqueous solution. This suggests that generation of Cl_2^- in solution may indeed occur according to reaction 1, avoiding previously mentioned shortcomings of reactions 3 and 4. While it remains to be seen if the same conclusion is applicable to the interfacial environment, in light of our results, this possibility should be given serious consideration, as we plan to do in our future work. As with the present calculations, we expect that high-level QM/MM methods will play an important role in clarifying inherent uncertainties of the exchange−correlation functional choice in DFT-based calculations for these sysems.

Acknowledgment. The work at Pacific Northwest National Laboratory (PNNL) was supported by the U.S. Department of Energy (DOE), Office of Basic Energy Sciences, Chemical Sciences, Geosciences, and Biosciences Division. Computational resources were provided by the Molecular Science Computing Facility (MSCF) in the William R. Wiley Environmental Molecular Sciences Laboratory (EMSL) funded by DOE's Office of Biological and Environmental Research. Battelle operates PNNL for the DOE under Contract DE-AC06-76RLO-1830. The work at UCI was supported in part by Grant CHE-0431512 from the National Science Foundation. Discussions with K. Kowalski and N. Govind are gratefully acknowledged.

References and Notes

(1) Jayson, G. G.; Parson, B. J.; Swallow, A. J. *J. Chem. Soc., Faraday Trans.* **1973**, *1*, 1597.
(2) Spicer, C.; Chapman, E.; Finlayson-Pitts, B.; Plastridge, R.; Hubbe, J.; Fast, J.; Berkowitz, C. *Nature* **1998**, *394*, 353–356.
(3) Knipping, E.; Lakin, M.; Foster, K.; Jungwirth, P.; Tobias, D.; Gerber, R.; Dabdub, D.; Finlayson-Pitts, B. *Science* **2000**, *288*, 301–306.
(4) Catton, R.; Symons, M. *J. Chem. Soc. A* **1969**, 446.
(5) Davis, M.; Koizumi, H.; Schatz, G. C.; Bradforth, S. E.; Neumark, D. M. *J. Chem. Phys.* **1994**, *101*, 4708–4721.
(6) Sevilla, M.; Summerfield, S.; Eliezer, I.; Rak, J.; Symons, M. *J. Phys. Chem. A* **1997**, *101*, 2910–2915.
(7) D'Auria, R.; Kuo, I. F. W.; Tobias, D. J. *J. Phys. Chem. A* **2008**, *112*, 4644–4650.
(8) Bartlett, R.; Musial, M. *Rev. Mod. Phys.* **2007**, *79*, 291.
(9) Kowalski, K.; Piecuch, P. *J. Chem. Phys.* **2001**, *115*, 643.
(10) Kowalski, K.; Piecuch, P. *Chem. Phys. Lett.* **2001**, *347*, 237.
(11) Valiev, M.; Garrett, B. C.; Tsai, M. K.; Kowalski, K.; Kathmann, S. M.; Schenter, G. K.; Dupuis, M. *J. Chem. Phys.* **2007**, *127*, 051102.
(12) Valiev, M.; Yang, J.; Adams, J. A.; Taylor, S. S.; Weare, J. H. *J. Phys. Chem. B* **2007**, *111*, 13455–13464.
(13) Valiev, M.; Bylaska, E. J.; Dupuis, M.; Tratnyek, P. G. *J. Phys. Chem. A* **2008**, *112*, 2713–2720.
(14) Berendsen, H. J. C.; Grigera, J. R.; Straatsma, T. P. *J. Phys. Chem.* **1987**, *91*, 6269–6271.
(15) Smith, D. E.; Dang, L. X. *J. Chem. Phys.* **1994**, *100*, 3757–3766.
(16) Vieceli, J.; Roeselova, M.; Potter, N.; Dang, L. X.; Garrett, B. C.; Tobias, D. J. *J. Phys. Chem. B* **2005**, *109*, 15876–15892.
(17) Francl, M.; Petro, W.; Hehre, W.; Binkley, J.; Gordon, M.; DeFrees, D.; Pople, J. *J. Chem. Phys.* **1982**, *77*, 3654.
(18) Dunning, T. H., Jr. *J. Chem. Phys.* **1989**, *90*, 1007.
(19) Henkelman, G.; Uberuaga, B. P.; Jonsson, H. *J. Chem. Phys.* **2000**, *113*, 9901–9904.
(20) Zhang, Y. K.; Liu, H. Y.; Yang, W. T. *J. Chem. Phys.* **2000**, *112*, 3483–3492.

JP903625K